Particle size and strain broadening in energy-dispersive x-ray powder patterns

Gerward, Leif; Mørup, Steen; Topsøe, Haldor

Published in:
Journal of Applied Physics

Link to article, DOI:
10.1063/1.322714

Publication date:
1976

Document Version
Publisher's PDF, also known as Version of record

Particle size and strain broadening in energy-dispersive x-ray powder patterns

L. Gerward

Laboratory of Applied Physics III, Technical University of Denmark, DK– 2800 Lyngby, Denmark

S. Mørup

Laboratory of Applied Physics II, Technical University of Denmark, DK– 2800 Lyngby, Denmark

H. Topsøe

Haldor Topsøe Research Laboratories, DK– 2950 Vedbaek, Denmark
(Received 30 June 1975; in final form 14 October 1975)

An energy-dispersive x-ray method for a rapid analysis of the broadening of diffraction lines in powder patterns has been developed. Experimental results are given for magnetite powders with sizes in the range 50–200 Å and compared with the results of standard angle-dispersive diffractometry and electron microscopy. The greatest advantages of the energy-dispersive method compared with the angle-dispersive method are the absence of the $K\alpha$ doublet, the simultaneous recording of a large part of the diffraction pattern, the fast data accumulation, and the adaptability of the technique to *in situ* studies. The method should be of special advantage for the study of solid-state reactions and processes such as sintering.

PACS numbers: 81.30.E, 61.10.

I. INTRODUCTION

The purpose of the present work is to introduce energy-dispersive x-ray diffraction for quantitative analysis of line broadening. Energy-dispersive diffraction, proposed in 1968,[1,2] has some unique advantages compared with standard angle-dispersive diffraction. The specimen is irradiated with a polychromatic x-ray beam; the photon energy spectrum of the x rays scattered through a fixed angle is measured by a semiconductor detector connected to a multichannel pulse-height analyzer. In this way several diffraction lines are recorded simultaneously, without any moving parts in the recording equipment.

In this work we have used direct measurements of linewidths to obtain information about crystallite size and microstrains. The method is illustrated by an experimental study of magnetite powders with particle sizes ranging from about 50 to 200 Å.

II. ENERGY-DISPERSIVE ANALYSIS OF LINE BROADENING

In energy-dispersive analysis Bragg's law is conveniently written in the form

$$Ed\sin\theta = \tfrac{1}{2}hc, \tag{1}$$

where E is the x-ray photon energy, d is the interplanar spacing, θ is the Bragg angle, h is Planck's constant, and c is the velocity of light. For practical purposes it is convenient to note that the constant on the right-hand side equals $\frac{1}{2}hc = 6.199$ keV Å if E is expressed in keV and d in Å.

Differentiating with respect to 2θ gives the relation between the line breadths measured on the 2θ scale used in angle-scanning diffraction and those measured on the energy scale used in this work:

$$\delta E = -\tfrac{1}{2}E\cot\theta\,\delta(2\theta). \tag{2}$$

Using Eqs. (1) and (2) the well-known formulas for the line breadths due to particle size, β_S, and distortions, β_D, in angle-dispersive diffraction[3] are transformed according to the following scheme:

$$\beta_S(2\theta) = \frac{K\lambda}{L\cos\theta}, \quad \beta_S(E) = \frac{K(\frac{1}{2}hc)}{L\sin\theta_0}, \tag{3a}$$

$$\beta_D(2\theta) = 4e\tan\theta, \quad \beta_D(E) = 2eE, \tag{3b}$$

where K is the Scherrer constant, λ is the x- ray wavelength, $2\theta_0$ is the fixed scattering angle, L is the average crystallite size, and e is the approximate upper limit of strain.

The combined size and strain broadening in the case of Gaussian profiles is given by

$$[\beta(E)]^2 = \left(\frac{K(\frac{1}{2}hc)}{L\sin\theta_0}\right)^2 + (2eE)^2. \tag{4}$$

The size and strain contributions can be separated by plotting $[\beta(E)]^2$ as a function of E^2. Available orders of a given reflection should give a linear plot with slope $4e^2$ and ordinate intercept $[K(\frac{1}{2}hc)/L\sin\theta_0]^2$ from which e and L can be calculated.

All information on the broadening effects is contained in the diffraction pattern taken at one fixed scattering angle. However, it may be useful to shift the positions of the diffraction peaks and record a number of diffraction patterns at different scattering angles. The scattering angle can be eliminated in Eq. (3a) using Eq. (1) and one obtains

$$\beta_S(E)/E = Kd/L. \tag{5}$$

From this relation it follows that the particle size can be calculated from the slope of a linear plot of $\beta_S(E)/E$ versus the lattice plane spacing for different orders of

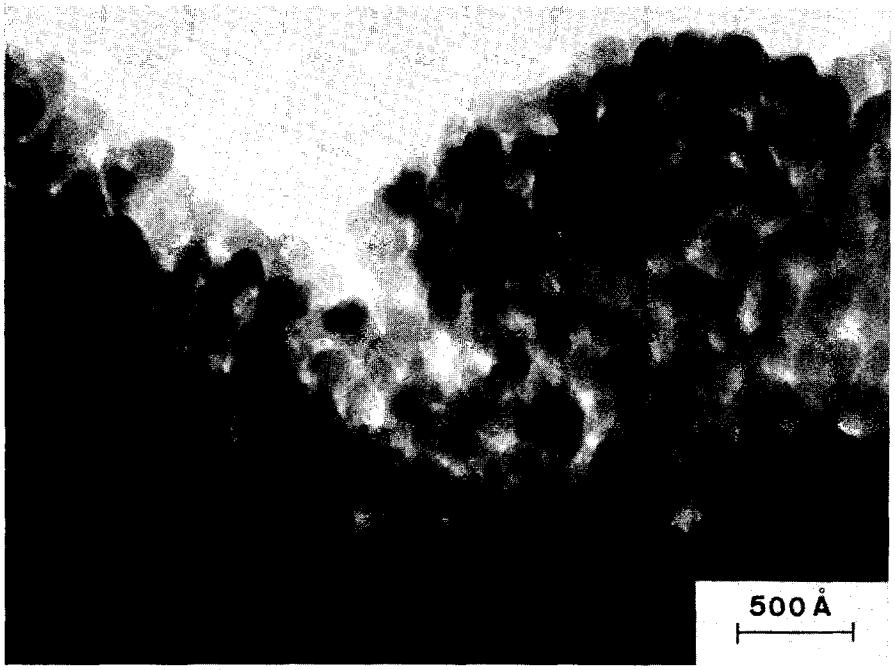

FIG. 1. Electron micrograph of sample No. 25-3.

a given reflection. Data taken at different scattering angles can be used in the same plot.

The instrumental broadening is due to the energy resolution of the detector and the angle resolution of the collimator. The latter part is obtained by inserting the angle divergence in Eq. (2). Useful energy resolution diagrams for typical Si(Li) and Ge(Li) detector systems have been published by Fukamachi, Hosoya, and Terasaki.[4] For two reasons it is desirable to make the angular part of the instrumental broadening smaller than the energy resolution of the detector: To avoid further broadening of the peaks and to avoid aberrations resulting in asymmetric peak shapes. These effects have been discussed in detail by Wilson.[5]

It is seen from Eq. (3a) that $\beta_S(E)$ is independent of energy but inversely proportional to $\sin\theta_0$. By choosing a small scattering angle one can get a large value of $\beta_S(E)$. A lower limit of the angle is set by the condition that the angular part of the instrumental broadening should be equal to or preferably smaller than the resolution of the detector. Consider, for example, a peak recorded at 30 keV. At this energy the resolution of our Si(Li) detector is about 300 eV (FWHM). The angular divergence of our collimating system is $\Delta\theta = 0.07°$. Insertion of this value in Eq. (2) shows that the angular part of the instrumental broadening equals 300 eV at $2\theta_0 = 14°$. Using this angle and assuming that the smallest broadening that can be observed is 10% of the resolution of the detector, one finds that it should be possible to measure particle sizes up to 1500 Å.

III. EXPERIMENTAL RESULTS

The magnetite samples were made by coprecipitation of a 2:1 molar mixture of a ferric and a ferrous salt in aqueous solution. An oxygen-free condition, which has been shown to be necessary,[6] was maintained during the experiments. All the samples were stoichiometric as

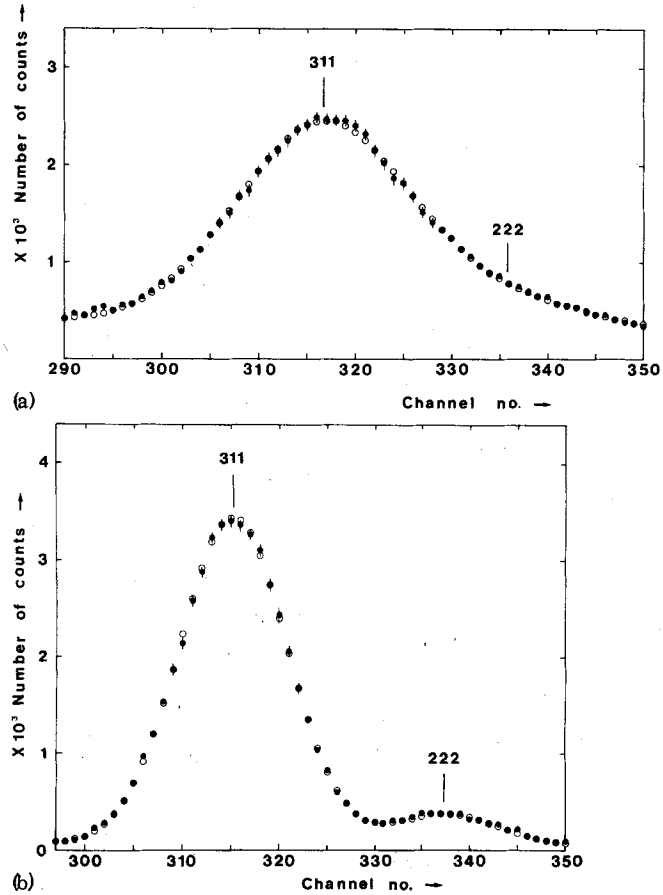

FIG. 2. Diffraction peaks on the photon energy scale fitted to Gaussian shape. Filled circles denote experimental points, open circles results of curve fitting. $2\theta_0 = 15°$. One channel corresponds to 37.2 eV. 3000 s counting time. (a) Sample No. 25-5. (b) Standard sample.

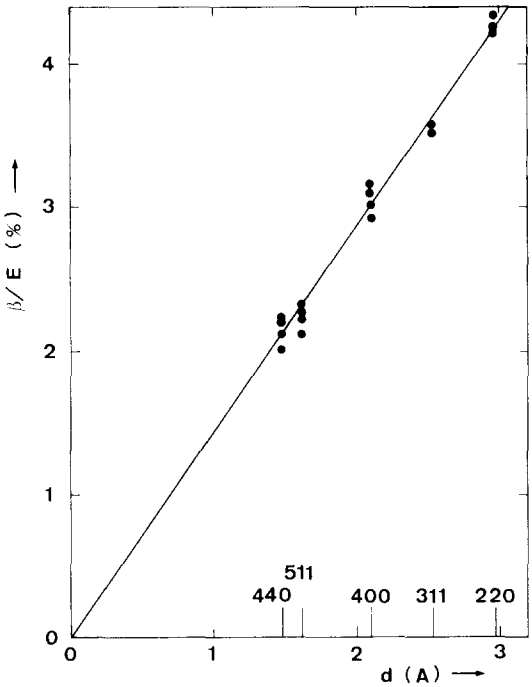

FIG. 3. Plot of particle-size broadening versus lattice plane spacing. Sample No. 25-5. The plot summarizes the results for a number of scattering anlges. ($2\theta_0 = 9°$, 12°, 15°, and 18°).

evidenced by the value of the lattice parameter and their Mössbauer spectra.[7]

Figure 1 shows an electron micrograph of magnetite powder with a particle size of about 160 Å. It is seen that the particles are very regular in shape (cubes or octahedra) and that the distribution of particle sizes is very narrow.

The diffraction peaks of the standard sample showing only instrumental broadening as well as the peaks of the samples showing broadening effects are very well described by a Gaussian shape (Fig. 2). The good agreement is expected since Gaussian line profiles can generally be used for a narrow size distribution. In this work we have used the half-maximum widths and we have set the Scherrer constant to $K = 0.9$.

The broadening, $\beta(E)$, of available orders of a given reflection has been found to be essentially independent of the photon energy. In a plot of $\beta(E)/E$ versus d (Fig. 3) the values for the 220 and 440 reflections define a straight line with zero intercept and the values of other reflections fall on the same line. This shows that no strain is present and that the particles are very regular in shape in agreement with the electron micrographs.

Table I summarizes the results of several methods used in this work to determine the particle size. The agreement between the crystallite sizes obtained by the two x-ray methods and the volume-average particle size obtained in the electron microscope is very good.

IV. CONCLUSIONS

It is seen in Sec. II that the theoretical expressions for the broadenings are very simple, expressed in terms of the x-ray photon energy, and that the size and strain contributions are easily separated.

TABLE I. Measured particle size in angstroms for a number of methods. The errors have been found from lines of maximum and minimum slope in diagrams like Fig. 3. The values obtained by electron microscopy are the volume-average particle sizes.

Sample No.	Energy-dispersive diffraction	Angle-dispersive diffraction	Electron microscopy
27-2	55 ± 5 [a]	54 ± 10	52 ± 8
25-5	63 ± 3 [b]	66 ± 10	71 ± 10
25-1	100 ± 20 [a]	110 ± 20	120 ± 20
25-3	150 ± 30 [a]	161 ± 30	190 ± 30

[a] Determined for $2\theta_0 = 12°$.
[b] Determined for $2\theta_0 = 9°$, 12°, 15°, and 18° (cf. Fig. 3).

The energy-dispersive detector records a large part of the diffraction pattern simultaneously and in a time much shorter than that required by an ordinary 2θ scan.

The appearance of the $K\alpha$ doublet in standard diffractometry leads sometimes to badly defined breadths unless complicated correction methods are employed. The direct observation of the diffraction breadth by the energy-dispersive method must be considered a significant simplification.

The diffraction peaks can easily be shifted on the energy scale by changing the scattering angle. The analogue operation in standard diffractometry is to change the wavelength, but there are only a few wavelengths available using standard x-ray tubes. Fluorescent radiation from the sample does not disturb the energy-dispersive analysis. The scattering angle can generally be chosen so that overlap of diffraction lines and fluorescence lines is avoided.

In energy-dispersive diffractometry the sample is fixed during an experiment. In addition, the path of the radiation is fixed by the choice of θ_0. Both of these features greatly facilitate construction of high- and low-temperature equipment and experiments on samples subjected to different controlled environments. The fast data acquisition makes the energy-dispersive method suitable for studies of solid-state reactions. Likewise processes such as sintering, which play an important role in catalysis and ceramics, can be followed continuously.

ACKNOWLEDGMENTS

The authors wish to thank B. Buras, A. Lindegaard Andersen, and J. Villadsen for helpful suggestions. They are also indebted to B. Ribe for technical assistance in the experiments and to O. Sørensen for taking the electron micrographs. Financial support from Statens teknisk-videnskabelige Fond is gratefully acknowledged.

[1] G. C. Giessen and G. E. Gordon, Science 159, 973 (1968).
[2] B. Buras, J. Chwaszczewska, S. Szarras, and Z. Szmid, Institute of Nuclear Research (Poland) Report No. 894/II/PS, 1968 (unpublished).

[3]H. P. Klug and L. E. Alexander, *X-Ray Diffraction Procedures*, 2nd ed. (Wiley, New York, 1974), Chap. 9.
[4]T. Fukamachi, S. Hosoya, and O. Terasaki, J. Appl. Crystallogr. **6**, 117 (1973).
[5]A. J. C. Wilson, J. Appl. Crystallogr. **6**, 230 (1973).
[6]H. Topsøe, J. A. Dumesic, and M. Boudart, J. Phys. **35**, C6-411 (1974).
[7]H. Topsøe and S. Mørup, *Proceedings of the International Conference on Mössbauer Spectroscopy, Kraków, Poland*, 1975 (AGH, Kraków, 1975), Vol. 1, p. 321.
[8]B. Buras, J. Staun Olsen, L. Gerward, B. Selsmark and A. Lindegaard Andersen, Acta Cryst. A**31**, 327 (1975).